

Performance of the Rangeland Hydrology and Erosion Model for runoff and erosion assessment on a semiarid reclaimed construction site

S.K. Nouwakpo, M. Weltz, M. Hernandez, T. Champa, and J. Fisher

Abstract: The ability to assess the impact of management actions on soil and water resources is crucial to sustainable land management. The Rangeland Hydrology and Erosion Model (RHEM) was developed as an assessment and decision support tool for resource management agencies and has been used to estimate soil erosion at national, regional, and local scales for both disturbed and undisturbed rangeland soil and vegetation conditions. In this paper, runoff, sediment, and microtopography data were collected during a series of rainfall simulation experiments aimed at evaluating the effectiveness of revegetation on a shrub-dominated post-construction hillslope where the soil has had time to reconsolidate. RHEM's input parameters are simple to collect and consist of soil texture, slope configuration, and canopy and ground cover. Experimental results showed that a mix of the shrub species rabbitbrush (*Chrysothamnus nauseosus*) and the invasive annual grass cheatgrass (*Bromus tectorum*) were more effective at reducing runoff and soil loss than rabbitbrush alone. Plots with more than 45% of residue cover produced as much as 2.1 times less runoff and 16 times less sediments than those with less than 15% of litter. Microtopographic changes information allowed partitioning the erosion process into diffuse and concentrated flow processes. Analysis of this 3D data highlighted the central role of concentrated flow erosion in sediment delivery on rangeland hillslopes. RHEM's performance as expressed by the coefficient of determination, R^2 , and the Nash-Stucliffe Efficiency (NSE) was $R^2 = 0.84$ and $NSE = 0.27$ for runoff and $R^2 = 0.81$ and $NSE = 0.26$ for sediments. This study demonstrates that RHEM can be effectively used by land managers and project managers to estimate soil erosion as a function of precipitation event on construction sites that have been revegetated to rangeland plant communities.

Key words: construction site—rangeland erosion—rangeland hydrology—reclamation—RHEM—soil erosion

Assessing the impact of management actions on water and soil resources with erosion and hydrological models is essential to sustainable land management. The estimated annual costs of damage caused by soil erosion and excessive sediment in surface waters within the United States is approximately US\$6 to US\$16 billion annually (Lal 1994; Osterkamp et al. 1998). Areas disturbed for construction activity have soil erosion rates from 2 to 40,000 times greater than preconstruction conditions and are important components of nonpoint source pollution that degrades surface water quality (Harbor 1999). In the United States, soil

erosion research was historically focused on addressing soil erosion issues on cropland leading to modeling tools ill-suited for conditions on rangelands (Nearing et al. 2011). Early attempts to apply empirical soil erosion models derived primarily from cropland data, such as the Universal Soil Loss Equation (USLE) and the Revised Universal Soil Loss Equation (RUSLE), on rangelands yielded unsatisfactory and contested results (Foster et al. 1981; Trieste and Gifford 1980).

The empirical model RUSLE was adapted and put forward as a tool to estimate long-term average annual soil loss on mining, construction, and reclamation sites (Renard

et al. 1997; Renard et al. 1991; Toy and Foster 1998). Toy et al. (1999) stated that significant errors may occur in soil loss estimates for a specific year or from a specific precipitation event when using RUSLE in this manner. Kaufman (2000), in his evaluation of 30 construction sites and multiple erosion control measures, reported that the poor performance in all categories of erosion control reflects a failure to integrate science and policy. He suggested a fundamental problem was the lack of basic data about soil, topography, and hydrology at the sites, leading to the incorrect application of practices to control hillslope scale soil erosion. There is a need for soil erosion tools that are designed to address specific return period precipitation events on both undisturbed and disturbed rangelands (postfire) and to assess rehabilitation efforts, such as revegetation of construction and mine reclamation projects.

The advent of physically based soil erosion models, such as the Water Erosion Prediction Project model (WEPP; Laffan et al. 1991), offered the opportunity to develop the scientific framework necessary to provide insight into the relationship between hydrologic processes and rangeland condition. In response to the need for an erosion and hydrology tool for rangeland, the Rangeland Hydrology and Erosion Model (RHEM) (Nearing et al. 2011) was developed from experimental data specifically collected on rangeland sites across the Western United States. As a process-based erosion model, RHEM models erosion and hydrology using the same fundamental principles as WEPP. Runoff generation and erosion on the hillslope are modeled in response to hydrological inputs and hydraulic parameters that are adjusted based on soil intrinsic properties and land surface conditions. On rangeland, hydrologic and erosion response is strongly controlled by the diversity and composition of vegetation life form (Pierson et al. 2002).

Sayjro Nouwakpo is a research professor in the department of Natural Resources and Environmental Science at the University of Nevada, Reno in Reno, Nevada. **Mark Weltz** is rangeland hydrologist and research leader at the Great Basin Rangeland Research Unit of the USDA Agricultural Research Service (ARS), Reno, Nevada. **Mariano Hernandez** is a hydrologist at the Southwest Watershed Research Center of the USDA ARS, Tucson, Arizona. **Tom Champa** is the Nevada state soil scientist and **John Fisher** is a senior regional soil scientist at the USDA Natural Resources Conservation Service, Reno, Nevada.

Consequently, RHEM estimates hydraulic parameters from knowledge of soil intrinsic properties, vegetation types (bunch grass, sod grass, annual grass, forbs, and shrubs) and management (represented as canopy and ground cover). The inclusion of vegetation type and management in the hydraulic parameter estimation confers a flexible framework to RHEM and allows its application to a wide range of rangeland conditions.

In the literature, RHEM has been applied to rangeland hydrology and erosion research on spatial scales ranging from hillslope process modeling (Belnap et al. 2013; Goodrich et al. 2011; Ross 2013; Weltz and Spaeth 2012) to regional scale resource and environmental assessment (Hernandez et al. 2013; Zhang et al. 2012). In most of these studies, RHEM was used to predict hydrology and erosion outcomes where limited observed data existed. Studies evaluating RHEM's prediction performance are limited due to the lack of experimental or monitoring data at the hillslope scale. To our knowledge, only Nearing et al. (2011) and Al-Hamdan et al. (2014) evaluated RHEM for runoff and soil loss prediction. Nearing et al. (2011) attributed the relatively weak performance of RHEM on soil loss prediction to the large variability typically obtained between replicates when soil erosion rates are extremely low. Since their study was conducted on undisturbed soils with low erosion rates, Nearing et al. (2011) pointed out the need for more evaluation of RHEM, especially on disturbed rangelands. RHEM was evaluated on rangeland sites disturbed by fire (Al-Hamdan et al. 2014). These authors proposed new concentrated flow erosion equations and a dynamic soil erodibility concept to improve short-term and long-term model performance on hillslopes disturbed by fire.

It is recognized that when rangeland landscapes undergo vegetation-reducing disturbances, soil erosion often increases. Pierson et al. (2009) found, for example, that immediately following prescribed-fire, loss of vegetation and soil property changes lead to increased erosion, especially to that caused by concentrated flow. This finding was further supported by Al-Hamdan et al. (2012) who reported postdisturbance increase in concentrated flow erodibility as high as 500-fold on burnt rangeland sites. Most rangeland management actions aimed at reducing soil erosion on rangeland are based on the

premise that exposed bare ground is directly linked to soil erosion. As a consequence, when rangeland landscapes are denuded by human activities, such as mining or construction, vegetation rehabilitation programs are often required to achieve specific postdisturbance outcomes (Audet et al. 2013). On rangeland, evaluation of ecosystem sustainability after a revegetation program may be enhanced by integrating ecological information (mainly resource needs) with hydrology and soil erosion predictions by means of an adequate modeling tool.

The aims of this study were to (1) assess the effect of vegetation and land surface characteristics on the hydrological and erosion response of a rehabilitated rangeland hillslope after disturbance by construction activities, and (2) use this experimental data to evaluate the performance of RHEM as a decision support system for postconstruction rehabilitation planning.

Materials and Methods

Study Site. The study area is located on a reclaimed construction site in Reno, Nevada, at the geographical location 39°34'22.65" N, 119°48'8.18" W and an average elevation of 1,495 m (4,905 ft). The soil is mapped as a complex of 75% Xman (clayey, smectitic, mesic, shallow Xeric Haplagids) and 25% rock outcrop mix. The Xman soil series is typically formed in hilly landforms from volcanic rock parent material. Because of the disturbance on this site, field soil surveys were specifically performed on this site for the purpose of this study. The top layer (0 to 15 cm [0 to 5.9 in]) is a very stony sandy loam soil with 5% clay content. From 15 cm to 30 cm (5.9 to 11.8 in) was the B horizon characterized by the accumulation of clay (>35%) in a mix of sand, stones, and large rocks and boulders. The soil profile below this depth was not explored during the field survey, but it was anticipated that the soil profile description below 30 cm will correspond to that of the generic Xman description (paralithic bedrock from 30 to 50 cm [11.8 to 19.7 in] and lithic bedrock below 50 cm). The drainage class at this site was classified as "well-drained" and the runoff class as "high," likely the result of the steep slopes.

The most recent construction operation on this site began in 2009 and ended with a rehabilitation effort in 2010. Figure 1 shows aerial images of the site before construction

(2007), immediately at the end of construction (2010), and two years after reclamation (2012). At the time of this study, the vegetation on the site was shrub-dominated (rabbitbrush [*Chrysothamnus nauseosus*]) with variable levels of annual grass incursion (cheatgrass [*Bromus tectorum*]).

A 900 m² (9,688 ft²) portion of the site was selected (red outline in figure 1) because (1) it was the area the most impacted by disturbance and (2) it presented a range of ground cover characteristics and slopes (18% to 30%), allowing a test of RHEM under various conditions.

Erosion Plots and Rainfall Simulation

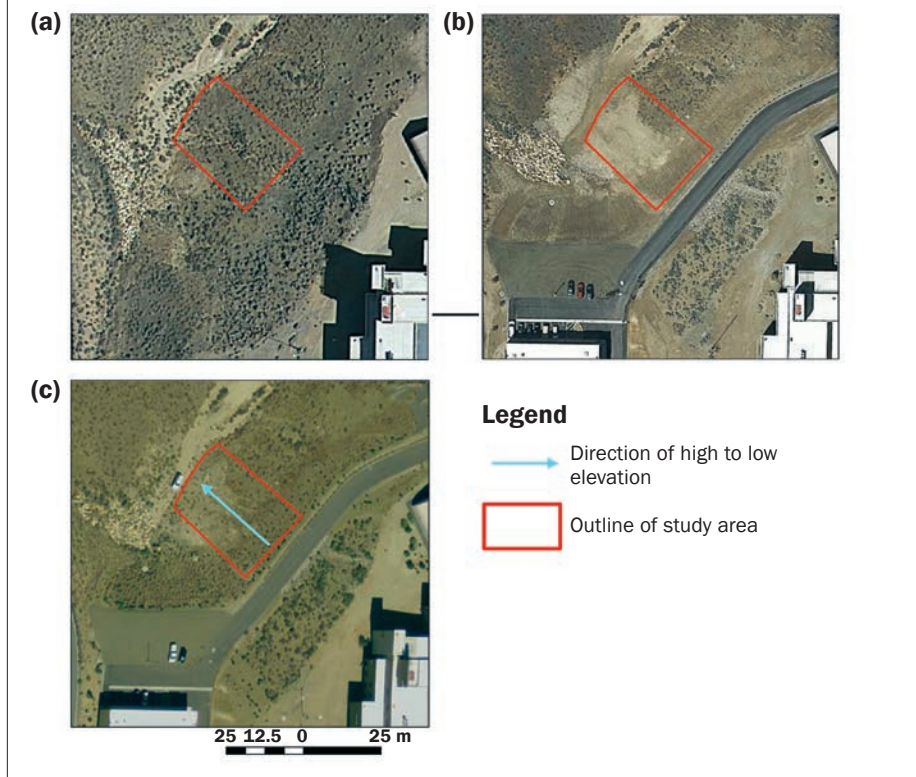
Experiment. Six 6 by 2 m (19.7 by 6.5 ft) erosion plots were selected on the study site to conduct rainfall simulation experiments. These experiments occurred during the summers of 2012 and 2013. Experiments were conducted on three plots (labeled 1, 2, and 3) in 2012 and three other plots (4, 5, and 6) in 2013 (figure 2). Plots were chosen to provide variability in slope and vegetation characteristics (table 1) for testing RHEM. Vegetation and ground cover were measured on each plot using a laser point frame (VanAmburg et al. 2005), and the average slope was calculated using a Nikon NPR 352 total station.

In our experimental conditions, many of the plot characteristics presented in table 1 were strongly correlated (table 2). It was desired to capture the effect of ground cover, canopy cover, and slope on hydrology and erosion processes. However, slope was negatively correlated with ground cover and positively with canopy cover because plots with the steepest slope (3, 5, and 6) were located at the top of the study hillslope where run-on from the adjacent parking lot promoted vegetation production. Therefore, two variables were selected for the sediment and runoff analyses in this study. Percentage of bare ground was selected to represent ground cover conditions, while grass canopy cover was selected to express independent live-vegetation influence on hydrologic and erosion processes because it was the variable the least correlated with ground cover.

On each plot, a series of rainfall simulation experiments were conducted to assess hydrologic and soil erosion responses. A Walnut Gulch Rainfall Simulator (WGRS) (Paige et al. 2004) was used for this study. The WGRS is composed of four VeeJet 80100 nozzles (Spraying Systems, Inc., Wheaton, Illinois)

Figure 1

Aerial image of the study site showing changes in vegetative cover over time [(a) 2007, (b) 2010, and (c) 2012] as a result of construction activities.



mounted along a central oscillating boom. The WGRS has an effective spray area of 6.1 by 2 m (20 by 6.5 ft), which determined the 6 by 2 m (19.7 by 6.5 ft) size of erosion plots used in this study. Rainfall application rate in this simulator is computer-controlled, allowing nominal intensities ranging from 12 to 200 mm h⁻¹ (0.47 to 7.87 in h⁻¹) at a nozzle pressure of 55 kPa (7.9 psi). A nozzle height of 2.44 m (8 ft) was respected in this study in accordance with recommendations of Paige et al. (2004).

On each plot, six rainfall intensities were applied: 13, 63, 101, 127, 152, and 190 mm h⁻¹ (0.5, 2.4, 3.9, 5, 5.9, and 7.4 in h⁻¹). Each simulation started with the lowest intensity (13 mm h⁻¹), which is a 15-minute wetting run designed to gradually increase and homogenize surface soil moisture content across plots. This procedure was expected to limit aggregate slaking due to rapid prewetting rate (Levy et al. 1997; Shainberg et al. 2003) and low antecedent soil moisture content (Truman et al. 1990). Assuming a porosity of 0.45 for the soil and neglecting capillary action, the 3 mm (0.1 in) of water applied during this wetting run occupied approximately a depth of 7 mm (0.3 in) of soil space, which is considered to

be larger than the active erosion layer in this study. On all the plots, this wetting run did not generate any runoff because the soil's infiltration rate was much greater than 13 mm h⁻¹ throughout the run. The subsequent rainfall intensities were applied from the smallest to the largest. After each rainfall event, a 30-minute wait time was observed to allow for the soil surface to drain to a subsaturation moisture content before the following run, thus homogenizing before-run soil moistures across plots. This wait time was also necessary to acquire photogrammetric images used for soil surface microtopography measurement.

The length of each simulated rainfall event varied based on the time required to initiate runoff. Once runoff was initiated, the simulation lasted 10 additional minutes (except for simulations on plot 4, which had to be prematurely interrupted for technical reasons) during which runoff and sediment data were collected. Runoff was conveyed through a supercritical flume where a Teledyne 4230 flow meter (Isco, Inc., Lincoln, Nebraska) measured discharge. Discharge measurements were made at a rate of four samples per minute, but averaged over the minute for analysis. Sediment samples were collected in

1 L (33.8 oz) bottles at one minute intervals. These bottles were immediately weighed and oven-dried, then reweighed to get sediment concentration in runoff.

Digital photogrammetry was used to generate high resolution (mm scale) Digital Elevation Models (DEMs) of the soil surface before and after each run. By subtracting elevation values before and after each run, soil erosion and deposition patterns were tracked within the plot (figure 3). Flow concentration pathways and rill geometry were also determined using this spatial information.

From the microtopographic data, a series of surface change metrics have been developed to characterize the response of soil surface to the erosion process. The total volumes of erosion *VolE* and deposition *VolD* are respectively the volumes of soil corresponding respectively to a loss and gain of elevation after an event and are computed using the following equations:

$$VolE = \sum(Z_{post} - Z_{pre}) \times \Delta x \times \Delta y | Z_{post} < Z_{pre}, \text{ and (1)}$$

$$VolD = \sum(Z_{pre} - Z_{post}) \times \Delta x \times \Delta y | Z_{post} > Z_{pre}, \text{ (2)}$$

where Z_{pre} and Z_{post} are the elevation values at a given DEM grid location before and after rainfall event, and Δx and Δy are the dimensions of a grid cell (5 mm [0.2 in] in this study).

The average depths of erosion *ZE* and deposition *ZD* are obtained by dividing *VolE* and *VolD* by the areas corresponding to erosion and deposition. Each difference of DEM was parsed into areas dominated by diffusive process (-10 mm [-0.4 in] < ΔZ < 5 mm [0.2 in]) and those that underwent concentrated flow processes ($\Delta Z \leq -10$ mm or $\Delta Z \geq 5$ mm). This method assumes that detachment and transport processes are greater in magnitude in concentrated flow pathways than they are in interrill areas. Therefore, the magnitude of microtopographic change resulting from concentrated flow processes should be distinguishable from that observed in areas where sheet and splash erosion dominate. The thresholds of -10 mm for erosion and 5 mm for deposition were chosen by iteratively testing various threshold values and selecting the ones that generated a realistic channel network with greater visual fidelity with field observations. Because elevation gains were systematically smaller in magnitude than elevation losses, a lower threshold magnitude was used for deposition compared to erosion

Figure 2

Orthophotos of erosion plots for visual assessment of vegetation composition and percentage of bare soil (BS).

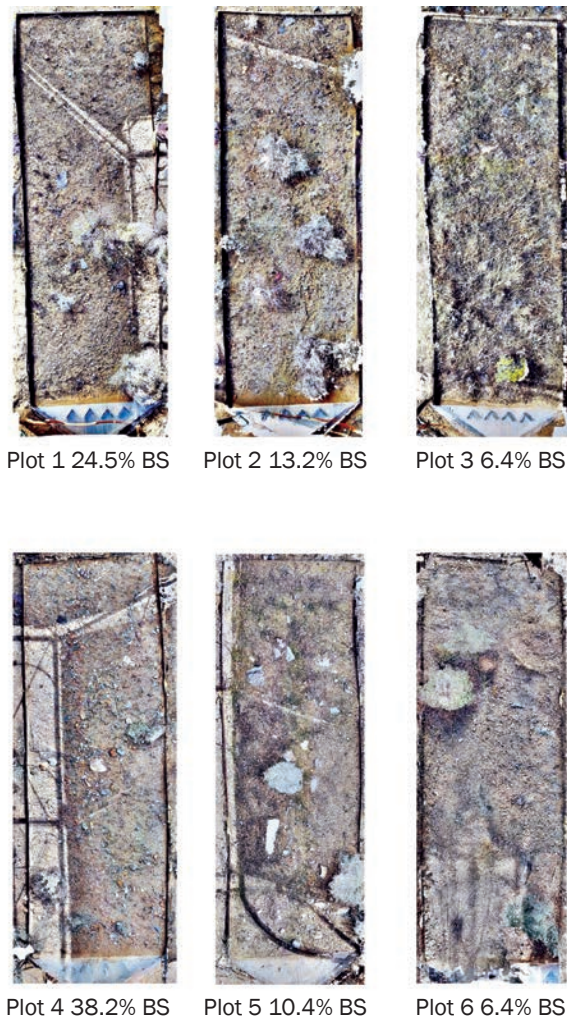


Table 1

Plot characteristic.

Plot ID	Ground cover (%)				Canopy (%)			Slope (%)
	Soil	Rock 2 to 5 mm	Rock ≥5 mm	Litter	Grass	Shrub	Total	
1	38.2	14.5	40.9	6.4	6.4	4.1	10.5	18
2	36.8	18.2	29.1	15.0	12.3	3.6	15.9	18
3	6.4	3.6	15.5	74.1	2.3	25.0	27.3	30
4	24.5	26.8	36.8	11.8	2.7	0.9	3.6	19
5	13.2	7.7	33.6	45.5	15.9	7.7	23.6	30
6	6.4	10.0	22.3	61.4	3.6	7.3	10.9	30

processes. Variables $VolE_c$, $VolD_c$, ZE_c , and ZD_c were then defined as the concentrated flow equivalent to their plot-wide counterparts.

To study the effect of various land and vegetation cover characteristics and hydrologic conditions on surface change metrics, a multiple linear regression was performed in the statistical software R (R Development Core Team 2015). Multiple regression for each surface change metric started with the following explanatory variables: bare soil, slope, rainfall duration, canopy cover, rainfall intensity, sediment concentration, runoff discharge, and cumulative runoff. A stepwise model selection by backward elimination was then performed to reduce the initial full model to the best-fitting model.

Due to the existing correlation between the explanatory variables, care was taken to avoid the problem of collinearity and unstable regression solution. To evaluate the stability of each regression model, condition numbers (Belsey et al. 1980) were estimated. Reduced models with condition numbers less than 30 were retained in this study. The high correlation between bare soil and slope in this study led to ill-conditioning when both variables were included in the same model. This problem was solved by applying a linear regression bare soil (BS) = f(Slope) and using its residuals in lieu of BS. It was also found that log-transforming surface change metrics resulted in improved prediction power.

Rangeland Hydrology and Erosion Model Parameterization. RHEM models runoff and erosion by adjusting process parameters to account for the diversity of soil properties and cover characteristics on rangelands. Among all the parameters internally used by RHEM, the ones requiring calibration for soil properties and vegetation characteristics are the friction factor (Fr), the Green-Ampt hydraulic conductivity (Ke), and the splash and sheet erodibility parameter (K_{ss}). RHEM provides estimation equations for Ke and K_{ss} based on the dominant rangeland vegetation community. Vegetation communities are divided into the following four categories: shrub, sod grass, bunch grass, and forbs. In our study, estimation equations corresponding to shrub communities in RHEM v2.2 (USDA ARS 2014) were used:

$$Ke = 28.8 \times e^{(0.3483[\text{basal_cover} + \text{litter_cover}])}, \text{ and} \quad (3)$$

$$K_{ss} = 2.6 \times 10^{(4.00836 - [1.17804 \times \text{rock_cover}] - [0.98186 \times \{\text{litter_cover} + \text{canopy_cover}\}])}. \quad (4)$$

Table 2
Correlation coefficients between plot variables.

Variable	Soil	Rock 2 to 5 mm	Rock ≥5 mm	Litter	Grass canopy	Shrub canopy	Total canopy	Slope
Soil	1.00							
Rock (2 to 5 mm)	0.63	1.00						
Rock (≥5 mm)	0.72	0.63	1.00					
Litter	-0.93	-0.82	-0.87	1.00				
Grass canopy	0.26	-0.11	0.32	-0.21	1.00			
Shrub canopy	-0.63	-0.79	-0.80	0.81	-0.29	1.00		
Total canopy	-0.45	-0.84	-0.58	0.66	0.35	0.79	1.00	
Slope	-0.95	-0.81	-0.68	0.94	-0.01	0.65	0.63	1.00

Figure 3

Example of rill width (red arrows) and rill spacing (black arrows) measurement from absolute change in elevation on plot 1 after the 190.5 mm h⁻¹ storm. The white holes in the map are outlines of shrub clumps removed before analysis.

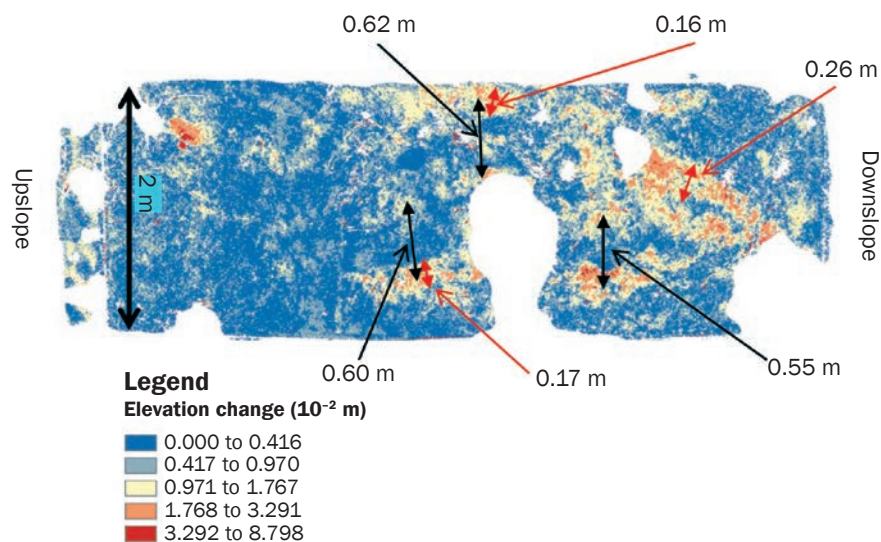


Table 3 shows RHEM parameters estimated for each plot.

Soil and surface intrinsic parameters (porosity, saturated fraction, rill spacing, and rill width) were maintained identical as model input for all experimental plots. By fixing these properties as model inputs for the study site, we assumed that soil intrinsic properties and hillslope dissection (into sheet and concentrated flow erosion areas) were uniform for the entire site and that differences in plot response were imputed to changes in vegetation and cover characteristics. This assumption was based on the premise that the recent disturbance of the study site may have reset soil and surface characteristics to uniform initial conditions.

In addition, because parameter estimation equations were not available in the official release of RHEM for these parameters, we decided to minimize across-plots variability in these variables.

Rill width (W) and rill spacing (R_s) were estimated from the maps of elevation differences after the 190.5 mm h⁻¹ (7.5 in hr⁻¹) event. The resulting difference maps were visually examined to determine areas of concentrated flow erosion (patches of substantially larger values than the diffuse background). Better results were obtained by performing the geometry measurement on the difference map rather than the delineated channel network because in the latter data, the network appeared discontinuous and network boundary ambiguous. Measurement of W and R_s

were made in the GIS software ArcGIS (ESRI 2011) at three transects in the lower half (figure 3) of each plot (table 4) and an overall site average determined. On plots 3, the very high litter cover from cheatgrass residues made accurate photogrammetric reconstruction impossible so this did not contribute to the W and R_s estimation. Average values for the site were $W = 0.17$ m (0.55 ft) and $R_s = 0.53$ m (1.7 ft).

Results and Discussion

Experimental Results. Figure 4 shows the hydrographs of each rainfall simulation of this study. The relatively stable runoff discharge following the increasing limb of the hydrograph suggests that a pseudo steady-state runoff was reached during each simulation. Table 5 summarizes erosion and hydrology response at steady state for each plot and rainfall intensity. Runoff rate increased with rainfall intensity for all plots. Discharge rate to rainfall intensity was not uniform across plots and was a function of plot vegetation characteristics and distribution.

In general, sediment concentration also increased with rainfall intensity (figure 5), consistent with the nonlinear relationship that is known to exist between detachment rate (especially splash and sheet erosion) and rainfall intensity. For the most erodible plot (Plot 1), an increase in sediment concentration was observed between 63 mm h⁻¹ (2.4 in hr⁻¹) and 152 mm h⁻¹ (5.9 in hr⁻¹) but followed by a decrease in soil loss at 190 mm h⁻¹ (7.5 in hr⁻¹). This decrease in sediment concentration after 152 mm h⁻¹ on Plot 1 was caused by the development of source limiting conditions on this plot as the high erosion rates it experienced depleted the most erodible soil fraction leading to surface armoring.

As was the case with runoff, sediment concentration also varied with plot characteristics. Both runoff and soil loss increased

Table 3
Estimated Rangeland Hydrology and Erosion Model parameters for each plot.

Plot ID	Friction factor (Fr)	Effective hydraulic conductivity (K_e [mm h ⁻¹])*	Interrill erodibility coefficient (K_{ss})*	Rill erodibility coefficient (K_c [s m ⁻¹])†	Rill critical shear stress (T_c [Pa]) †	Rill spacing (R_s [m])	Rill width (W [m])
1	4	29	1,209	0.004	1.12	0.53	0.17
2	5	30	1,156	0.004	1.12	0.53	0.17
3	46	37	718	0.004	1.12	0.53	0.17
4	5	30	1,345	0.004	1.12	0.53	0.17
5	16	33	886	0.004	1.12	0.53	0.17
6	29	35	856	0.004	1.12	0.53	0.17

*Equations 3 and 4.

†Manually calibrated for the test site to best-fit observed data.

Table 4
Concentrated-flow-paths distribution and geometry estimated from changes to soil surface microtopography.

Plot ID	Number of flow paths	Average channel width (m)	Channel spacing (m)
1	4	0.20	0.59
2	4	0.17	0.32
3	—	—	—
4	3	0.17	0.69
5	3	0.15	0.52
6	3	0.19	0.45
Average	3.4	0.17	0.53

with percentage of bare soil (figures 6a and 6b). Table 6 lists for each rainfall intensity regression coefficients obtained by fitting a linear model between bare-soil and steady-state runoff and erosion. Data suggest that increasing ground cover with litter, for example, promotes infiltration by increasing surface roughness, thereby reducing flow velocity but dramatically reduces erosion by shielding soil from raindrop kinetic energy. As an example, for the most erosive event in our study, a decrease of bare ground from the 38.2% to 6.4% resulted in a 1.3-fold reduction in runoff while sediment flux was reduced by a factor of 15.

The effect of grass canopy cover (mainly cheatgrass) on runoff and soil erosion shown in figures 6c and 6d does not suggest any consistent trend. For all but the 190 mm h⁻¹ (7.5 in hr⁻¹) intensity, an initial increase in runoff and soil loss with grass cover was followed by a decrease beyond 15% of grass cover. A decrease in runoff and sediment is normally expected based on known interactions between grass ecosystems and erosion and runoff generation processes. In our study the limited number of data points (six in total) and the existence of correlation between

many hillslope characteristics (table 2) likely confounded the relationship between grass canopy and hydrology erosion processes.

Erosion Processes from 3D Data. Table 7 presents volumes and average depths of erosion and deposition estimated from the 3D reconstructions before and after each event. In figure 7, estimated volumes of erosion, deposition, and net erosion ($VolE - VolD$) are plotted against observed cumulative soil loss. Observed soil losses explained 40% and 25% of variabilities in $VolE$ and net erosion volumes, but were weakly coupled with deposition processes, explaining only 4% of $VolD$. In addition, in some cases, net erosion volumes were negative for small sediment losses, likely the result of 3D measurement errors and changes in bulk density during deposition. The conversion of topographically estimated erosion volumes into masses of sediment often lead to soil losses with little relation to observed values (Heng et al. 2010; Nouwakpo and Huang 2012; Rieke-Zapp and Nearing 2005) due to factors such as raindrop-induced changes in bulk density, the selective detachment of fine particles, and the marginal contribution of the soil colloidal fraction to microtopography.

Nevertheless, topographically derived erosion and deposition volumes can be used to improve understanding on processes and factors controlling the response of land surface to erosive events (Nouwakpo and Huang 2012).

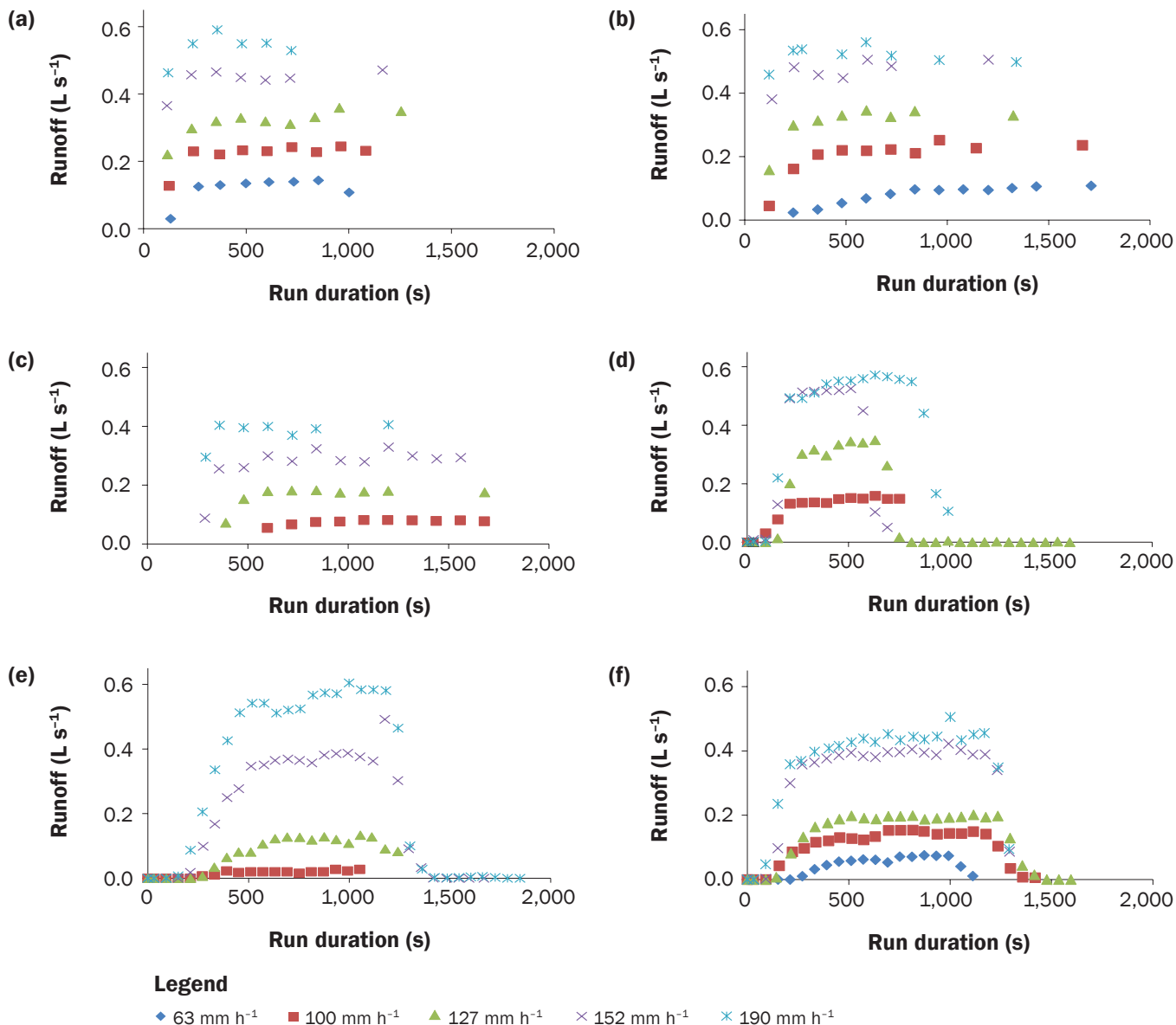
Results of the multiple regressions are presented in table 8. The multiple regressions explained a larger variance of $VolE$ and $VolD$ compared to the simpler linear model with soil loss in figure 7, suggesting that both masses of soil loss and changes to soil surface microtopography are products of complex interactions between erosive processes and land surface characteristics, but result in outcomes that are not equivalent. $VolE$ shows a statistically significant effect of runoff discharge, but the negative regression coefficient might be the result of the development of source limiting conditions. In addition to the effect of runoff discharge, $VolE_c$ shows a significant and increasing effect of sediment concentration and canopy cover. This result highlights the central role of concentrated flow pathways in sediment production and delivery to hillslope outlet.

$VolD$ was positively related to runoff discharge, likely the result of the development of source-limiting condition and possibly armoring of the soil surface with less transportable particles left after successive rainfall events. The surface armoring theory was further supported by the positive effect of runoff duration and cumulative runoff on $VolD_c$. These positive effects of runoff duration and cumulative runoff on $VolD$ and $VolD_c$ also suggest that areas that are undergoing deposition are less likely to be reentrained within a given rainfall-runoff event.

The normalization of erosion of deposition volumes by areas improved the R^2 of the multiple regressions for plot-wide surface change metrics, but did not substantially change R^2 for the channel processes.

Figure 4

Hydrograph of rainfall simulation experiments ([a] plot 1, [b] plot 2, [c] plot 3, [d] plot 4, [e] plot 5, and [f] plot 6). Plots 3 and 5 did not generate runoff for the 63 mm h⁻¹ event, while plot 2 produced runoff for this intensity, but the data is missing.



Overall plot area may vary slightly between plots during the manual cropping of the 3D data along the plot perimeter, leading to the improved R^2 after normalization. ZE was mainly controlled by the percentage of bare soil and cumulative runoff. As bare soil increased, more areas of the plot were subjected to sheet and splash erosion, thus increasing volumes of erosion per unit area. Cumulative runoff also had an increasing effect on ZE .

In channels, variables with statistically significant effects on ZE_c were slope, canopy, and

sediment concentration. Here again, the positive effect of sediment concentration highlights the importance of channels in hillslope sediment production and delivery, and this is further supported by the negative effect of sediment concentration on sheet erosion contribution. Canopy now has a negative effect on ZE_c while its effect on $VolE_c$ was positive. This suggests that vegetation might inherently structure runoff into many flow concentration pathways of low flow capacities, thus reducing downcutting. Nevertheless, overall contribution of concentrated flow erosion in total erosion increased

with bare ground as illustrated by the significant negative effect of bare soil in sheet erosion contribution. As slope increased, channels deepened, a result of increased runoff flow hydraulics and consistent with current concentrated flow erosion theories.

ZD showed statistically significant and positive effects of bare soil and cumulative runoff. The positive effect of bare soil on ZD demonstrates that sediment availability controls redistribution along the hillslope. The positive effect of cumulative runoff on both ZD and ZD_c further support the previous observation

Table 5
Observed and Rangeland Hydrology and Erosion Model (RHEM)-predicted runoff and erosion response from the rainfall simulation experiments.

Plot ID	Intensity (mm h ⁻¹)	Rainfall duration (s)	Cumulative runoff (L)	Observed		RHEM predictions		
				Sediment flux (kg m ⁻² h ⁻¹)	Runoff (mm h ⁻¹)	Sediment flux (kg m ⁻² h ⁻¹)	Sheet erosion (kg m ⁻² h ⁻¹)	Runoff (mm h ⁻¹)
1	63	894.59	118.24	0.14	40.17	0.04	0.04	35.88
1	100	1,005.32	228.56	0.71	73.63	1.80	0.11	74.02
1	127	1,206.65	382.98	2.18	95.12	3.24	0.17	99.43
1	152	1,171.64	528.34	5.19	143.04	4.57	0.24	124.85
1	190	678.36	182.70	4.51	182.01	6.41	0.36	162.97
2	63	1,777.92	129.88	0.06	28.28	0.04	0.04	40.07
2	100	1,645.24	340.00	1.33	67.41	0.80	0.11	78.20
2	127	1,319.15	403.74	2.20	100.72	1.97	0.17	103.61
2	152	1,208.73	550.34	3.38	148.01	3.05	0.23	129.02
2	190	1,323.06	651.02	4.44	160.74	4.09	0.35	167.14
3	63	1,014.28	0.00	0.01	22.75	0.03	0.03	38.73
3	100	1,930.99	126.02	0.02	23.36	0.07	0.07	77.06
3	127	1,407.50	242.75	0.02	55.10	0.10	0.10	102.68
3	152	1,961.98	568.60	0.32	86.41	0.14	0.14	127.63
3	190	981.75	365.62	0.12	121.26	0.22	0.22	165.73
4	63	—	—	—	—	—	—	—
4	100	687.10	96.92	0.32	43.32	1.31	0.12	75.40
4	127	536.35	164.13	0.78	102.56	2.63	0.19	100.81
4	152	405.59	299.61	2.82	151.31	3.84	0.27	126.22
4	190	472.51	218.56	2.20	158.27	5.53	0.40	164.34
5	63	—	0.00	0.00	0.00	0.03	0.03	38.86
5	100	747.68	15.67	0.00	5.06	0.08	0.08	76.82
5	127	995.82	60.74	0.02	36.05	0.13	0.13	102.23
5	152	704.65	205.48	0.10	109.83	0.37	0.18	127.63
5	190	717.11	327.13	0.15	153.42	1.40	0.27	165.74
6	63	707.07	43.58	0.03	21.63	0.03	0.03	38.77
6	100	692.04	86.34	0.09	39.00	0.08	0.08	76.82
6	127	687.97	124.27	0.13	53.43	0.12	0.12	102.22
6	152	717.01	276.71	0.60	118.80	0.17	0.17	127.63
6	190	711.34	283.81	0.86	126.87	0.26	0.26	165.73

that areas undergoing deposition might not be reentrained unless erosivity is increased.

Rangeland Hydrology and Erosion Model Simulation Result. Figures 8a and 8b show runoff rate and soil loss predictions by RHEM plotted against observed values. As illustrated by the relatively large R^2 values obtained for runoff (0.84) and sediments (0.81), patterns in observed data were captured by the RHEM model. The Nash-Stucliff Efficiency (NSE), which measures the agreement between observed and predicted data, was $NSE = 0.27$ for runoff and $NSE = 0.26$ for soil loss. Figure 8a shows a bias in predicted runoff rates expressed as the nonzero intercept of the regression equation, likely the result of underestimated infiltration rates. The slope of the regression equation for runoff was also less than 1, suggesting that RHEM's runoff response to rainfall intensity was dampened by other factors. Overall, in our experimental conditions, low runoff events (<140 mm h⁻¹ [5.5 in hr⁻¹]) were

Figure 5
Average sediment concentration measured during each simulation. N/A signifies missing data, while an absent bar means 0 g L⁻¹.

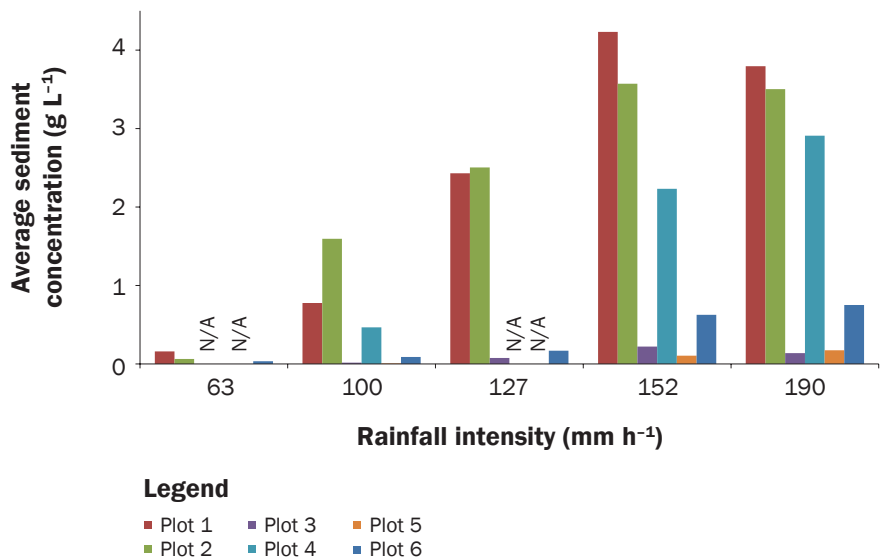
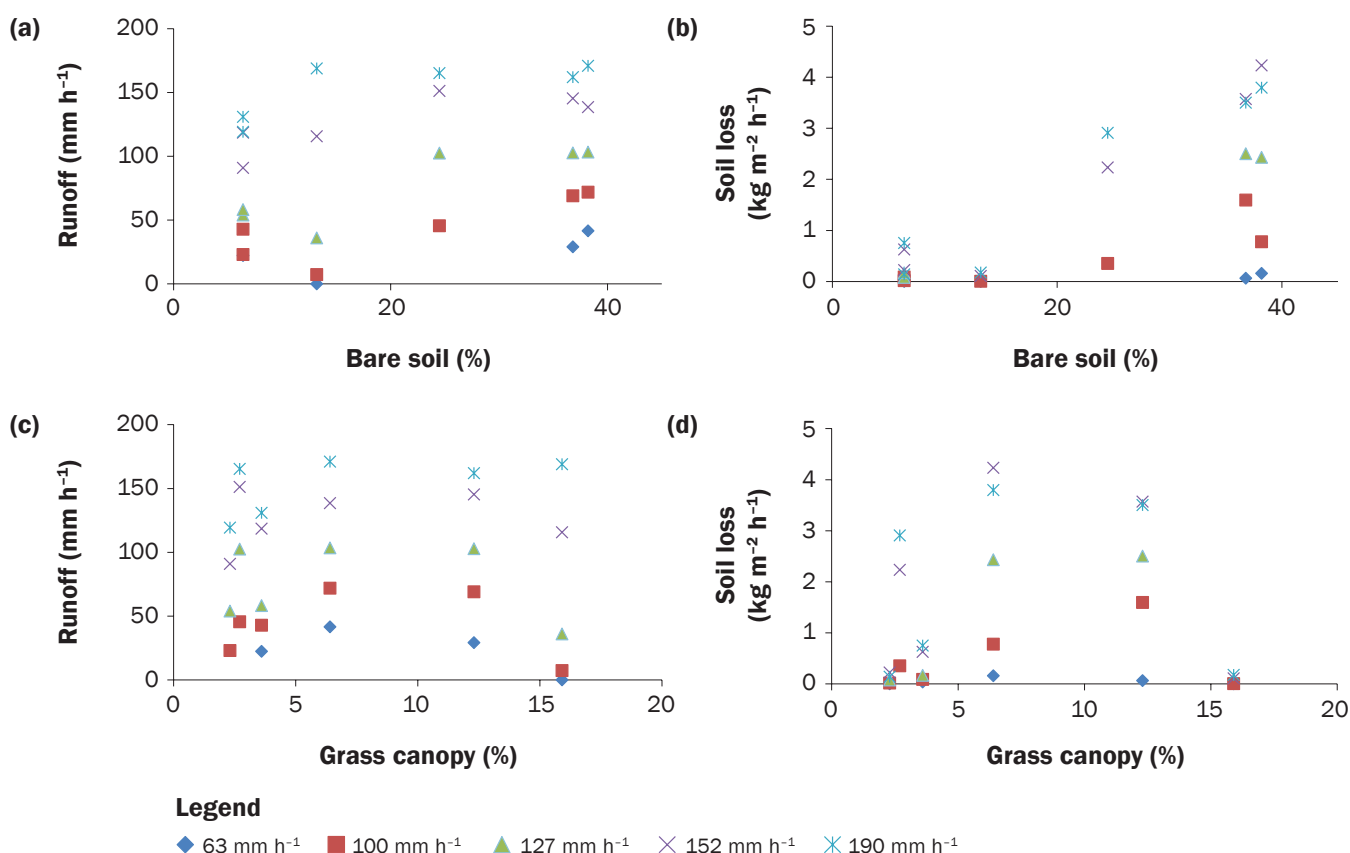


Figure 6

Steady-state (a and c) runoff rate and (b and d) soil loss as a function of percentage of (a and b) bare soil and (c and d) grass canopy.



overestimated while high runoff events ($\geq 140 \text{ mm h}^{-1}$) were slightly underestimated.

For soil loss (figure 8b), the regression intercept was nearly zero and its slope close to one, suggesting that little bias was present in the soil loss data and that RHEM's soil loss response to rainfall intensity was consistent with that observed in the measured data. Overall, agreement between observed and predicted soil losses gradually deviates from the 1:1 line from small to large erosion rates.

Previous evaluation of RHEM (Nearing et al. 2011) resulted in NSE values of 0.83 and 0.21 for runoff and sediment prediction, respectively, with R^2 values of 0.87 and 0.50. The better performance of RHEM at predicting runoff in Nearing et al. (2011) can be attributed to the fact that this model was applied to undisturbed rangelands with similar plot characteristics as those used to develop RHEM. Nevertheless, the high runoff R^2 obtained in our study suggests that patterns in runoff were accurately detected, but new parameter estimation equations affecting infiltration processes (mainly the

Table 6

Slopes, intercept, and coefficient of determinations (R^2) of the linear models between bare soil (BS) and steady-state runoff and erosion in figure 6.

Intensity	Runoff	Soil loss
63	$0.763\text{BS} + 5.227,$ $R^2 = 0.50$	$0.003\text{BS} - 0.016,$ $R^2 = 0.66$
100	$1.427\text{BS} + 13.426,$ $R^2 = 0.67$	$0.037\text{BS} - 0.298,$ $R^2 = 0.73$
127	$1.798\text{BS} + 38.541,$ $R^2 = 0.74$	$0.075\text{BS} - 0.358,$ $R^2 = 1.00$
152	$1.255\text{BS} + 100.470,$ $R^2 = 0.64$	$0.119\text{BS} - 0.667,$ $R^2 = 0.93$
190	$1.134\text{BS} + 129.174,$ $R^2 = 0.55$	$0.112\text{BS} - 0.472,$ $R^2 = 0.90$

effective hydraulic conductivity K_e) are needed to accommodate our disturbed site. RHEM's soil loss prediction performance in our study was comparable to that of Nearing et al. (2011) (NSE = 0.26 versus 0.20), but with larger R^2 in our study (0.81 versus 0.50).

The improved R^2 in our study is likely due to the wide range of erosion rates obtained from our disturbed site contrasting with the small soil losses on the undisturbed test sites used in Nearing et al. (2011).

Table 7
Soil loss and surface change metrics estimated from 3D reconstruction.

Plot ID	Intensity (mm h ⁻¹)	Plot-wide processes				Concentrated flow processes				Soil loss (g)*
		VoIE (m ³)	VoID (m ³)	ZE (m)	ZD (m)	VoIE _c (m ³)	VoID _c (m ³)	ZE _c (m)	ZD _c (m)	
1	63	0.022	0.002	0.003	0.001	0.001	0.001	0.012	0.008	375.04
1	100	0.027	0.009	0.004	0.003	0.004	0.005	0.014	0.008	2,068.10
1	127	0.015	0.012	0.003	0.002	0.003	0.003	0.014	0.007	7,666.64
1	152	0.027	0.009	0.004	0.003	0.007	0.004	0.015	0.008	12,034.15
1	190	0.012	0.034	0.004	0.005	0.004	0.023	0.016	0.009	3,939.99
2	63	0.013	0.017	0.003	0.003	0.001	0.007	0.014	0.008	324.56
2	100	0.030	0.009	0.004	0.003	0.008	0.005	0.014	0.008	6,961.80
2	127	0.021	0.011	0.004	0.003	0.004	0.004	0.013	0.008	9,556.45
2	152	0.018	0.018	0.003	0.004	0.002	0.011	0.014	0.009	9,123.98
2	190	0.040	0.008	0.006	0.003	0.015	0.004	0.014	0.008	14,041.58
3	63	—	—	—	—	—	—	—	—	0.00
3	100	—	—	—	—	—	—	—	—	134.48
3	127	—	—	—	—	—	—	—	—	392.42
3	152	—	—	—	—	—	—	—	—	1,436.72
3	190	—	—	—	—	—	—	—	—	438.38
4	63	—	—	—	—	—	—	—	—	—
4	100	0.007	0.009	0.001	0.001	0.000	0.001	0.013	0.007	769.68
4	127	0.003	0.013	0.001	0.001	0.000	0.001	0.013	0.006	—
4	152	0.011	0.005	0.001	0.001	0.000	0.001	0.014	0.007	4,658.38
4	190	0.008	0.011	0.001	0.002	0.000	0.002	0.013	0.007	3,610.10
5	63	—	—	—	—	—	—	—	—	—
5	100	—	—	—	—	—	—	—	—	9.23
5	127	0.016	0.025	0.003	0.003	0.003	0.011	0.015	0.008	—
5	152	0.016	0.012	0.003	0.002	0.002	0.003	0.013	0.007	184.66
5	190	0.005	0.027	0.002	0.003	0.000	0.008	0.013	0.007	344.61
6	63	0.011	0.015	0.002	0.003	0.002	0.005	0.016	0.009	64.07
6	100	—	—	—	—	—	—	—	—	182.07
6	127	0.023	0.009	0.003	0.003	0.003	0.003	0.018	0.010	340.01
6	152	0.007	0.025	0.003	0.003	0.001	0.007	0.016	0.007	1,371.12
6	190	0.011	0.014	0.002	0.002	0.001	0.004	0.016	0.008	1,599.64

*Measured from sediment samples.

Observed and predicted runoff and soil loss data are shown in figure 9 for each erosion plot. Figure 9 suggests that RHEM adequately responded to increase in rainfall intensity for runoff and erosion predictions. The influence of increased litter cover on plots 3, 5, and 6 on soil erosion rates was accurately predicted by RHEM (i.e., lower sediment production). However, interplot patterns in runoff response were less accurately captured by RHEM as plots 3, 5, and 6 produced as much runoff as the other plots in the model outputs. In other words, there was a notable effect of litter cover on runoff rate in the observed data, but RHEM was less sensitive to this effect.

Effect of Vegetation and Slope on Soil Erosion Processes. For most of the western United States semiarid rangelands and especially the Great Basin sagebrush steppe, cheatgrass is an invasive species associated with increased fire frequency and ecosystem degradation (Pierson et al. 2011). Long-term erosion risk on cheatgrass-invaded sites

Figure 7
Erosion and deposition volumes estimated from 3D reconstruction as a function of soil loss.

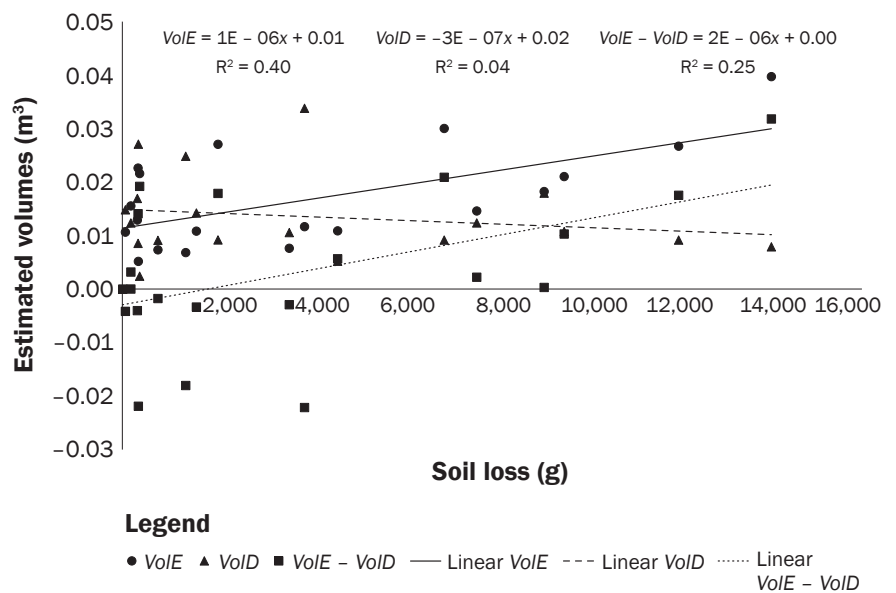


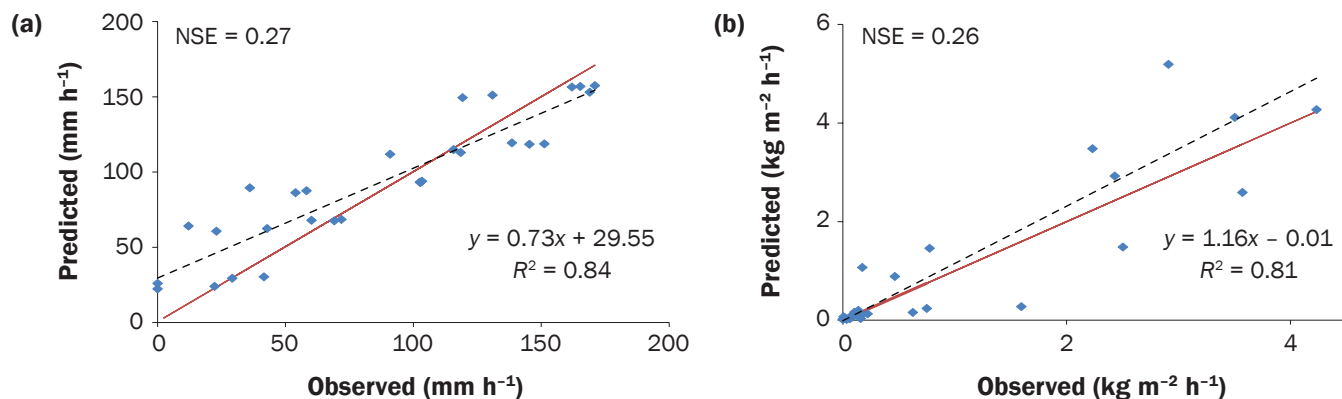
Table 8
Multiple regression on surface change metrics using hydrology and plot characteristics.

Explained variable	Plot-wide processes			Concentrated flow processes		
	Explanatory variables	Coefficient, p-value†	ANOVA p-value†	Explanatory variables	Coefficient, p-value†	ANOVA p-value†
$VolE_c$ $R^2 = 0.65$ $R^2 = 0.67^*$	Intercept	0.0149, 0.0129		Intercept	-9.76, 2.73×10^{-8}	
	Canopy	0.000454, 0.110	0.0843	Bare soil	-3.22, 0.0712	0.0594
	Sediment concentration	0.000393, 0.166	0.00197	Canopy	0.252, 0.001.32	0.00949
	Runoff discharge	-0.0502, 0.00308	0.0117	Sediment concentration	0.1.16, 0.000332	0.00112
	Cumulative runoff	1.34×10^{-5} , 0.0594	0.0594	Runoff discharge	-3.58, 0.0384	0.0384
$VolD_c$ $R^2 = 0.31$ $R^2 = 0.48^*$	Intercept	0.0106, 0.0110		Intercept	-9.69, 7.87×10^{-8}	
	Bare soil	0.000696, 0.0772	0.158	Slope	10.7, 0.00559	0.153
	Sediment concentration	-0.000382, 0.0665	0.423	Runoff duration	0.00125, 0.0193	0.0134
	Runoff discharge	0.0270, 0.0423	0.0423	Cumulative runoff	0.0008.02, 0.0241	0.0241
ZE_c $R^2 = 0.82$ $R^2 = 0.66^*$	Intercept	0.00226, 0.00488		Intercept	-4.81, 2.70×10^{-16}	
	Bare soil	8.30×10^{-5} , 0.0288	7.24×10^{-6}	Bare soil	0.009.52, 0.1.35	0.757
	Runoff duration	7.18×10^{-7} , 0.190	0.00277	Slope	2.50, 7.70×10^{-5}	0.00706
	Runoff discharge	-0.00328, 0.0568	0.0513	Runoff duration	0.000130, 0.0429	0.415
	Cumulative runoff	1.70×10^{-6} , 0.00269	0.00269	Canopy	-0.0159, 0.00833	0.00411
				Sediment concentration	0.00514, 0.0128	0.0128
ZD_c $R^2 = 0.57$ $R^2 = 0.45^*$	Intercept	0.00346, 2.83×10^{-5}		Intercept	-4.79, 1.44×10^{-15}	
	Bare soil	8.46×10^{-5} , 0.0285	0.00178	Slope	0.830, 0.172	0.605
	Runoff coefficient	-0.00217, 0.0504	0.986	Intensity	-0.00161, 0.117	0.406
	Cumulative runoff	1.19×10^{-6} , 0.00750	0.00750	Runoff coefficient	-0.229, 0.211	0.237
				Cumulative runoff	0.000209, 0.00484	0.00484
Sheet erosion $R^2 = 0.60$	Intercept	1.10, 5.42×10^{-9}				
	Bare soil	-0.00990, 0.0115	0.00201			
	Slope	-0.719, 0.0722	0.528			
				Sediment concentration	-0.00713, 0.00245	0.00245

*Coefficients of determination R^2 values for channel processes.

†Values in bold font highlight statistical significance at 5% confidence level.

Figure 8
Rangeland Hydrology and Erosion Model predictions for steady-state (a) runoff rate and (b) soil loss against observed data. The red line indicates the line of perfect agreement (1:1 line).



results from the increased fire susceptibility (Weltz et al. 2014b). In this study, we found that plots with high litter content as the result of cheatgrass invasion were less susceptible to erosion and produced less runoff. In an urban or semiurban setting, cheatgrass invasion could be beneficial for hillslope stability and off-site erosion reduction if fire risks are carefully controlled. It is worth noting that the high density of cheatgrass on plots 3, 5, and 6 was facilitated by the added run-on from the adjacent impervious surface, so management plans should consider water availability for urban revegetation designs.

When vegetation became sparse in this study, concentrated flow processes became increasingly critical to sediment production and delivery to plot outlet. Landscape evolution studies in arid climatic regimes have determined that accelerated soil erosion has resulted from changing from a wet, moist climate to drier, warmer climate across the southwestern United States (Bull and Schick 1979; Miller et al. 2001; Wells et al. 1987). These observations led to the development of a process-response model to explain the relationship between decreasing precipitation and increased soil erosion at the hillslope scale. Bull and Schick (1979) hypothesized that changes in climate altered the effective precipitation, which resulted in a corresponding change in vegetation with a reduction in grass and forb understory and an open shrub community. This open shrub community had a decreased vegetative canopy cover and a corresponding increase in bare ground. We found in our study that increased bare ground was accompanied by an increased contribution of concentrated flow erosion to total erosion volumes. In addition, our study found that these flow concentration pathways are efficient sediment delivery features, leading to significant sediment loading in runoff, and perhaps exacerbating land degradation as precious resources are exported off-site.

Slope was also found in our study to control the magnitude of concentrated flow erosion processes with enhanced channel downcutting when slope was increased. Deep channels in these sparsely vegetated landscapes might lead to rapid drainage of subsurface water reserves and potentially accentuate desertification. Carroll et al. (2000) evaluated slope, type of vegetation, and native bare soil versus spoils to determine soil erosion and water quality impacts with various mine reclamation techniques.

They reported that the greatest risk of soil erosion was before vegetation was established. If rainfall occurs during this stage, then it is likely that rills will form and concentrated flow induced soil erosion will be greatly accelerated. If vegetation does not eventually establish in these rills, then soil erosion will continue to accelerate as the rills become persistent and increase in depth and width. Carroll et al. (2000) determined that risk of soil erosion and transport of salt and other contaminants are directly related to the slope of the rehabilitated site.

Complementing observed soil loss measurement with 3D surface change data in this study provided a unique insight into interactions and feedback that may exist between erosion processes and vegetation. We found that increase in vegetation canopy promoted the structuring of runoff in many concentrated flow pathways, but of low capacity. This finding is consistent with currently hypothesized vegetation-surface process interaction theories. Numerous authors have discussed the importance of vegetation-driven hydrologic connectivity in controlling runoff and sediment movement at the hillslope scale (Mueller et al. 2007; Reaney et al. 2007; Reid et al. 1999). These authors and numerous others proposed that vegetation patterns control hydrologic connectivity and hillslope erosion on rangelands (Dunkerley and Brown 1999; Imeson and Prinsen 2004; Tongway and Ludwig 1997; Valentin et al. 1999). Dominant erosion processes vary with rangeland conditions, the type of plants present, the gap between plant basal areas, and the connectivity of the bare interspaces (Okin et al. 2009). Plant basal areas, rocks, litter, woody debris, and biological soil crusts prevent soil loss from occurring from raindrop splash by protecting the soil surface from impact (Belnap 2006). These obstructions will cause water to flow around them, resulting in concentrated soil erosion in the interspace areas (Ludwig et al. 2007; Puigdefabregas 2005). This process results in an island effect where excessive soil erosion occurs in the interspace area where runoff is concentrated (Ravi et al. 2010). The erosion-site degradation process can be accelerated in these situations and result in loss of biotic integrity, desertification, and sustainability of the site and transport of contaminants off site in the runoff water (Carroll et al. 2000; Chartier and Rostagno 2006; Ridolfi et al. 2008; Schlesinger and Pilmanis

1998; Schlesinger et al. 1996). Examples of this is often seen in shrub dominated landscapes that have formed coppice dunes (e.g., sagebrush [*Artemisa spp.*], creosotebush [*Larrea spp.*], and mesquite [*Prosopis spp.*]) and in woodlands where Juniper (*Juniperus spp.*) and Pinyon Pine (*Pinus spp.*) have expanded into sagebrush steppe communities in arid and semiarid rangelands (Davenport et al. 1998; Pierson et al. 1994, 2011; Spaeth et al. 1994).

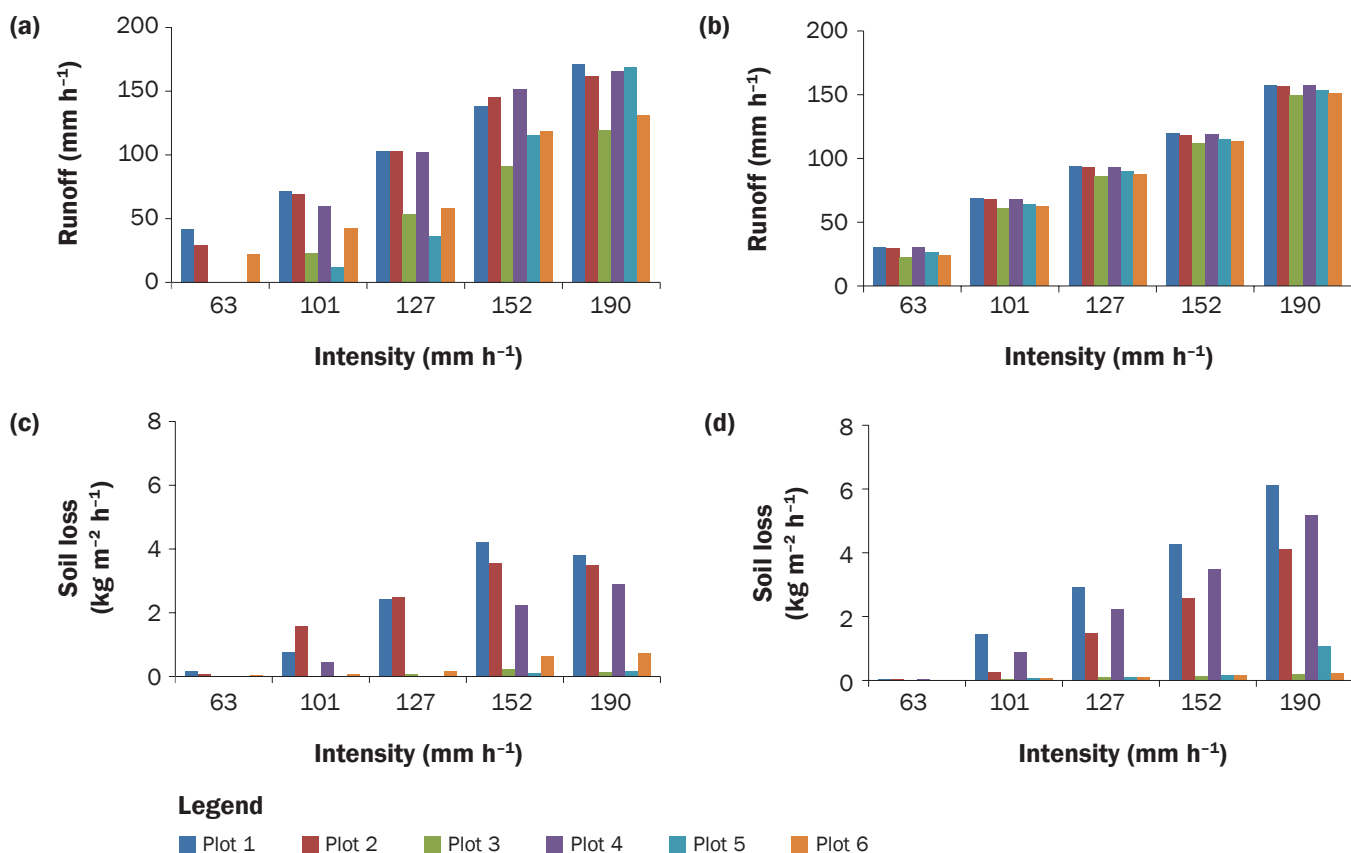
Rangeland Hydrology and Erosion Model as Decision-Support System for Land Reclamation Planning. The key to minimizing soil erosion in rehabilitation projects is to have adequate spatial distribution of vegetation and litter to reduce rainfall splash erosion and concentration of rill and gully-forming overland flow. When addressing urban or semiurban rehabilitation planning, such as postconstruction revegetation efforts, it is critical to determine the necessary cover to prevent accelerated soil erosion. The rehabilitation plan should address both average vegetative and ground cover and also the spatial distribution of the cover distribution down slope to prevent concentrated flow from accumulating. It is not only the total vegetative canopy and ground cover, but the spatial distribution of cover, plant density, and basal gaps between plants that needs to be controlled to prevent concentration flow accumulation, rill formation, and accelerated soil erosion.

Our study showed that the influence of land surface conditions, namely litter cover, on soil loss, was well represented within RHEM, while interplot runoff patterns were less accurately predicted. More research is certainly needed to improve RHEM's runoff sensitivity to ground cover on disturbed hillslopes and provide more adequate parameter estimation equations for rangelands disturbed by construction and mining activities. With respect to soil erosion, figure 10 shows that RHEM-estimated concentrated flow erosion in this study did not match those approximated with the 3D data, and the discrepancies worsened on low ground cover.

Recent studies (Al-Hamdan et al. 2013; Pierson et al. 2008, 2009; Pierson et al. 2010; Williams et al. 2014) have identified concentrated flow erosion to be the dominant erosion process on disturbed rangelands. RHEM was initially developed from intact rangelands in which concentrated flow erosion might be marginal, and this may explain the absence of parameter estimation equations for concentrated flow erosion processes in the official release of RHEM. This

Figure 9

(a and c) Observed and (b and d) predicted steady-state (a and b) runoff rates and (c and d) soil loss.



lack of detail on rangeland concentrated flow erosion processes has prompted some authors (Al-Hamdan et al. 2014) to develop specific parameter estimation equations for concentrated flow erosion prediction when rangelands are in disturbed conditions. The enhancements made by Al-Hamdan et al. (2014) addressed disturbances by fire and tree encroachment, but it is still unclear the extent to which these improvements can be expanded to other rangeland disturbances. Perhaps a more fundamental question to ask is whether the lack of understanding of concentrated erosion processes stems from the inadequacy of conventional soil erosion measurement techniques in partitioning soil erosion into diffuse (sheet and splash) and concentrated flow erosion. In this study, the use of 3D data was useful at parsing erosion into its components, and more research is needed to further clarify the magnitude and role of concentrated flow erosion in both pristine and disturbed rangeland conditions.

RHEM is built on a flexible framework allowing the estimation of model parameters

using equations that are specific to rangeland soil and conditions. As a decision support tool, this model structure is highly advantageous because it alleviates the otherwise data-expensive and time-consuming step of model calibration. Many model users (e.g., land users and managers, regulation agencies, etc.) who use these hydrologic models do not have the time or the data required for accurate model calibration and validation. Nevertheless parameter refinement is useful and sometimes necessary in instances where observed data are available and high fidelity between observed and model prediction is sought. For research purposes, estimation equations in RHEM can be used to find appropriate initial values for hydraulic and hydrologic parameters that can be further refined to better fit specific land conditions; however, care must be taken to bound parameters within the range of values consistent to prevailing rangeland conditions.

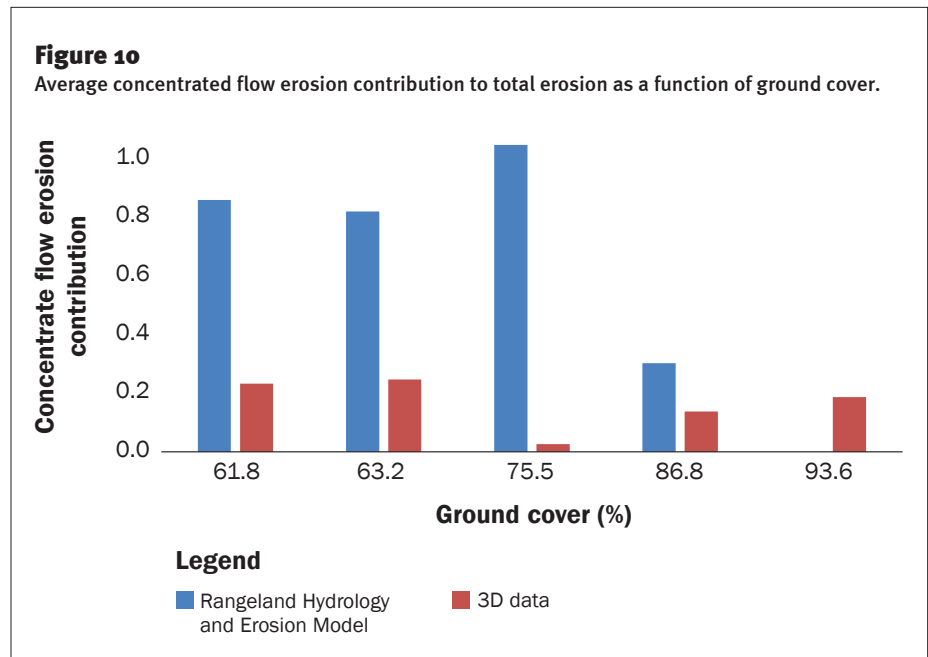
In our study, the parameter refinement strategy mentioned above would have been useful to improve runoff and erosion prediction in RHEM. In RHEM, rangeland

communities are divided into the following four categories: shrub, sod grass, bunch grass, and forbs. Parameter estimation equations are specifically derived for each of these vegetation communities. In our study, equations corresponding to shrub vegetation were used. A possible approach to parameter optimization would be to calculate model parameters corresponding to each vegetation community for the specific land surface conditions on each plot. This information can then be used to bound parameter values to ranges consistent with shrub vegetation communities. To model infiltration processes, for example, RHEM uses the Green-Ampt Mein Larson model (Mein and Larson 1971) and estimates the soil hydraulic conductivity based on vegetation characteristics, soil intrinsic properties, and ground cover. As suggested by the bias in the regression equation of figure 8a, estimated K_e values using these equations were systematically smaller than the actual values. In addition, refinement to K_{ss} , K_c , and T_c would have improved sheet and splash and concentrated flow ero-

sion predictions. However, this step was not taken due to the relatively small sample size in this study (six plots) in comparison to the number of parameters (four) to be refined and the potentially confounding effect of the successive rainfall experimental protocol used in this study.

In a management scenario where the focus is on runoff volume control, RHEM would have provided over-estimated runoff values for plots with high ground cover. Nevertheless, in urban and semiurban environments, the focus is rarely on runoff because hydraulic structures are typically designed to handle large runoff volumes resulting from high-magnitude-low-frequency (HMLF) events on impervious surfaces. If the focus is on soil erosion, however, RHEM would have accurately predicted the erosion reduction benefit of the abundance of vegetation residue due to the presence of the annual grass in the shrub community, and perhaps this vegetation mix would have been systematically adopted for revegetation. In addition, RHEM can be used in combination with the weather generation tool Cligen (Nicks et al. 1995) to simulate hillslope response to events of specific return periods, providing users with the ability to perform scenario analyses and risk assessments.

In our study, the 63, 100, 127, 152, and 190 mm h⁻¹ (0.5, 2.4, 3.9, 5, 5.9, and 7.4 in hr⁻¹) rainfall intensities applied correspond respectively to 61, 268, 577, 1,026, and 2,096 year return storms (based on a 15-minute storm duration) for the area of interest (figure 11). HMLF events are the primary runoff generation mechanisms on rangelands (Cooper 1967; Renard 1970). Annual average soil loss are often low on rangelands, but damage caused by (HMLF) events can trigger dramatic changes in ecological conditions (Weltz et al. 2014a). Our results suggest that concentrated flow erosion plays a strong control on hillslope sediment delivery by contributing to the detachment and transport process and shortening the path of sediment from source areas to hillslope outlet. On sparsely vegetated rangelands, the occurrence of HMLF increases the likelihood of channel formation and hillslope fragmentation. Once these channels are formed, they rapidly increase hydrologic connectivity during subsequent events and promote resource exports with potentially significant ecological consequences. In addition, in an urban setting, knowledge



of hydrological response to HMLF events is useful in the design of infrastructures for managing runoff and sediments loads.

RHEM predicted a marked increase of concentrated flow contribution to total erosion beyond the 63 mm h⁻¹ (2.4 in hr⁻¹) storm (61 year return period; figure 12). This trend was not consistent with estimated contributions from the 3D data, perhaps a consequence of the disturbance that the study hillslope has undergone. Nevertheless, such a dramatic increase in concentrated flow erosion might be consistent with the crossing of a threshold beyond which channels become actively eroding on intact rangeland hillslopes. From a management perspective, the adverse effects of this increase in potential channel erosion can be dampened by increasing vegetation cover. In our study, plots 3, 5, and 6, which were the most affected by the cheatgrass invasion, produced the least amount of runoff and sediments. Taking the hillslope as a whole, these three plots were located near the top of the hillslope where run-on from the paved adjacent surface facilitated vegetation production. In turn, this vegetation promotes further reduction in runoff and sediment delivery to downslope less vegetated (and thus more vulnerable) surfaces. This feedback mechanism naturally occurs in sparsely vegetated landscape and manifests itself as banded vegetation patterns (Dunkerley and Brown 1999; Saco et al. 2007; Valentin et al. 1999; Wilcox et al. 2003). Perhaps a hillslope management plan that minimizes the exacerbating effect of concentrated flow

erosion during HMLF events might be to promote a mosaic of heterogeneous hillslope elements functionally linked in this source-sink coupling.

It is important to note that parameter estimation equations developed for RHEM version 2.2 were used in this paper, but these equations have been recently succeeded by version 2.3. In addition, concentrated flow processes were modelled in our study using the shear stress concept. The most current version of RHEM uses the stream power concept after Al-Hamdan et al. (2012) suggested a better performance of this parameter compared to the shear stress. This new version of RHEM has not been tested on our data, but it is anticipated that our conclusions on runoff predictions will remain the same since estimation equations for *Ke* are the same as in version 2.2.

Summary and Conclusions

Rainfall simulation experiments were conducted on a shrub-dominated hillslope to evaluate postconstruction rehabilitation efforts. Experiment results showed that runoff and erosion decreased with ground cover. Plots with more than 45% of residue cover produced as much as 2.1 times less runoff and 16 times less sediments than those with less than 15% of litter. Changes to soil surface microtopography were monitored during each rainfall event. This microtopographic data allowed gaining insight into interactions between land surface condition (vegetation cover and slope) and sediment transport processes. Results of the 3D data

analysis highlighted the central role of concentrated flow erosion in sediment delivery on rangeland hillslopes. We also found that vegetation (expressed as canopy cover) structured runoff into many pathways of low flow erosivity. RHEM was evaluated by comparing model outputs to observed data. Relatively large R^2 values obtained for runoff (0.84) and sediments (0.81) predictions suggest that patterns in observed data were captured by the RHEM model. Estimated model efficiencies were $NSE = 0.27$ for runoff and $NSE = 0.26$ for soil loss. However, detailed analyses of RHEM's predictions suggest that the effect of ground cover on soil loss was adequately captured by the model, but with dampened runoff response.

RHEM can be applied as a decision support tool with limited inputs to evaluate the impact of alternative revegetation practices and determine the amount of change in vegetation and ground cover that is required to reduce accelerated soil erosion from given runoff events to a desired level. More research is needed to clarify the role of ground cover on infiltration processes and provide better estimation equations for rangeland sites disturbed by construction or mining activities.

References

- Al-Hamdan, O.Z., M. Hernandez, F.B. Pierson, M.A. Nearing, C.J. Williams, J.J. Stone, J. Boll, and M.A. Weltz. 2014. Rangeland hydrology and erosion model (RHEM) enhancements for applications on disturbed rangelands. *Hydrological Processes* 29(3):445-457.
- Al-Hamdan, O.Z., F.B. Pierson, M.A. Nearing, C.J. Williams, J.J. Stone, P.R. Kormos, J. Boll, and M.A. Weltz. 2012. Concentrated flow erodibility for physically based erosion models: Temporal variability in disturbed and undisturbed rangelands. *Water Resources Research* 48.
- Al-Hamdan, O.Z., F.B. Pierson, M.A. Nearing, C.J. Williams, J.J. Stone, P.R. Kormos, J. Boll, and M.A. Weltz. 2013. Risk assessment of erosion from concentrated flow on rangelands using overland flow distribution and shear stress partitioning. *Transactions of the American Society of Agricultural and Biological Engineers (ASABE)* 56:539-548.
- Audet, P., S. Arnold, A.M. Lechner, and T. Baumgartl. 2013. Site-specific climate analysis elucidates revegetation challenges for post-mining landscapes in eastern Australia. *Biogeosciences* 10:6545-6557.
- Belnap, J. 2006. The potential roles of biological soil crusts in dryland hydrologic cycles. *Hydrological Processes* 20:3159-3178.
- Belnap, J., B.P. Wilcox, M.W. Van Scoyoc, and S.L. Phillips. 2013. Successional stage of biological soil crusts:

Figure 11

Empirically estimated return frequency of the simulated rainfall intensities, assuming 15-minute duration (Bonnin et al. 2006).

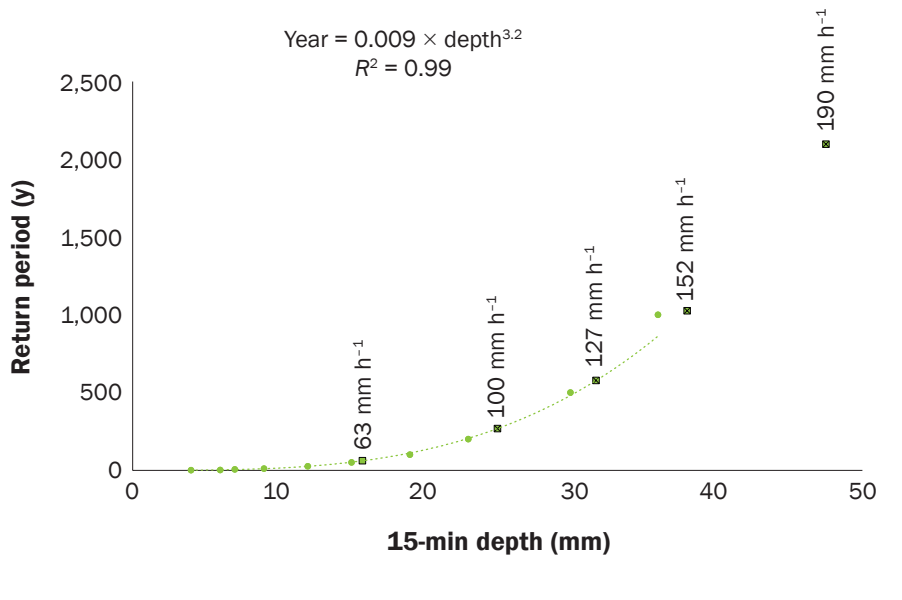
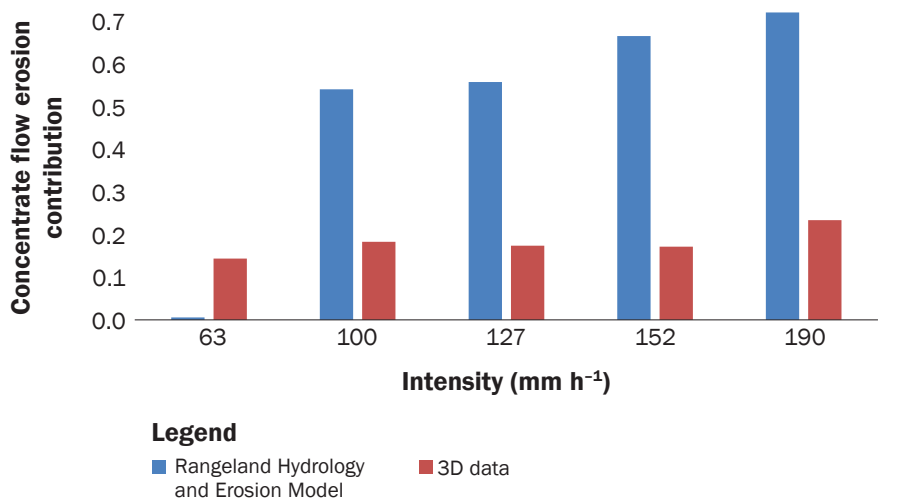


Figure 12

Average concentrated flow contribution to total soil loss as a function of intensity.



- An accurate indicator of ecohydrological condition. *Ecohydrology* 6:474-482.
- Belsey, D.A., E. Kuh, and R.E. Welsch. 1980. Regression diagnostics: Identifying influential data and sources of collinearity. New York: Wiley.
- Bonnin, G.M., D. Martin, B. Lin, T. Parzybok, M. Yekta, and D. Riley. 2006. Precipitation-frequency atlas of the United States. NOAA atlas 14(2).
- Bracken, L.J., and J. Croke. 2007. The concept of hydrological connectivity and its contribution to understanding runoff-dominated geomorphic systems. *Hydrological Processes* 21:1749-1763.

- Bull, W.B., and A.P. Schick. 1979. Impact of climatic change on an arid watershed: Nahal Yael, southern Israel. *Quaternary Research* 11:153-171.
- Cammeraat, L.H. 2002. A review of two strongly contrasting geomorphological systems within the context of scale. *Earth Surface Processes and Landforms* 27:1201-1222.
- Cammeraat, E.L.H. 2004. Scale dependent thresholds in hydrological and erosion response of a semiarid catchment in southeast Spain. *Agriculture, Ecosystems and Environment* 104:317-332.
- Carroll, C., L. Merton, and P. Burger. 2000. Impact of vegetative cover and slope on runoff, erosion, and

- water quality for field plots on a range of soil and spoil materials on central Queensland coal mines. *Australian Journal of Soil Research* 38:313-327.
- Chartier, M.P., and C.M. Rostagno. 2006. Soil erosion thresholds and alternative states in northeastern Patagonian rangelands. *Rangeland Ecology and Management* 59:616-624.
- Cooper, C.F. 1967. Rainfall intensity and elevation in southwestern Idaho. *Water Resources Research* 3:131-137.
- Davenport, D.W., D.D. Breshears, B.P. Wilcox, and C.D. Allen. 1998. Viewpoint: Sustainability of piñon-juniper ecosystems—A unifying perspective of soil erosion thresholds. *Journal of Range Management* 51:231-240.
- Dunkerley, D.L., and K.J. Brown. 1999. Banded vegetation near Broken Hill, Australia: Significance of surface roughness and soil physical properties. *Catena* 37:75-88.
- ESRI (Environmental Systems Research Institute). 2011. ArcGIS Desktop Release 10. Redlands, CA: Environmental Systems Research Institute.
- Foster, G.R., J.R. Simanton, K.G. Renard, L.J. Lane, and H.B. Osborn. 1981. Application of the Universal Soil Loss Equation to rangelands on a per-storm basis – Discussion. *Journal of Range Management* 34:161-165.
- Goodrich, D.C., D.P. Guertin, I.S. Burns, M.A. Nearing, J.J. Stone, H. Wei, P. Heilman, M. Hernandez, K. Spaeth, F. Pierson, G.B. Paige, S.N. Miller, W.G. Kepner, G. Ruyle, M.P. McClaran, M. Weltz, and L. Jolley. 2011. AGWA: The Automated Geospatial Watershed Assessment tool to inform rangeland management. *Rangelands* 33:41-47.
- Harbor, J. 1999. Engineering geomorphology at the cutting edge of land disturbance: Erosion and sediment control on construction sites. *Geomorphology* 31:247-263.
- Heng, B.C.P., J.H. Chandler, and A. Armstrong. 2010. Applying close range digital photogrammetry in soil erosion studies. *Photogrammetric Record* 25:240-265.
- Hernandez, M., M.A. Nearing, J.J. Stone, F.B. Pierson, H. Wei, K.E. Spaeth, P. Heilman, M.A. Weltz, and D.C. Goodrich. 2013. Application of a rangeland soil erosion model using National Resources Inventory data in southeastern Arizona. *Journal of Soil and Water Conservation* 68(6):512-525, doi:10.2489/jswc.68.6.512.
- Imeson, A.C., and H.A.M. Prinsen. 2004. Vegetation patterns as biological indicators for identifying runoff and sediment source and sink areas for semiarid landscapes in Spain. *Agriculture, Ecosystems and Environment* 104:333-342.
- Kaufman, M.M. 2000. Erosion control at construction sites: The science-policy gap. *Environmental Management* 26:89-97.
- Lafren, J.M., L.J. Lane, and G.R. Foster. 1991. WEPP—A new generation of erosion prediction technology. *Journal of Soil and Water Conservation* 46(1):34-38.
- Lal, R. 1994. Global Overview of Soil Erosion. In *Soil and Water Science: Key to Understanding Our Global Environment*, ed. R.S. Baker, G.W. Gee, and C. Rosenzweig, p. 39-51. Madison, WI: Soil Science Society of America.
- Levy, G.J., J. Levin, and I. Shainberg. 1997. Prewetting rate and aging effects on seal formation and interrill soil erosion. *Soil Science* 162:131-139.
- Ludwig, J.A., R. Bartley, A.A. Hawdon, B.N. Abbott, and D. McJannet. 2007. Patch configuration non-linearly affects sediment loss across scales in a grazed catchment in north-east Australia. *Ecosystems* 10:839-845.
- Mein, R.G., and C.L. Larson. 1971. Modeling the infiltration component of the rainfall-runoff process. Minneapolis, MN: Water Resources Research Center, University of Minnesota.
- Miller, J., D. Germanoski, K. Waltman, R. Tausch, and J. Chambers. 2001. Influence of late Holocene hillslope processes and landforms on modern channel dynamics in upland watersheds of central Nevada. *Geomorphology* 38:373-391.
- Mueller, E.N., J. Wainwright, and A.J. Parsons. 2007. Impact of connectivity on the modeling of overland flow within semiarid shrubland environments. *Water Resources Research* 43:13.
- Nearing, M.A., H. Wei, J.J. Stone, F.B. Pierson, K.E. Spaeth, M.A. Weltz, D.C. Flanagan, and M. Hernandez. 2011. A rangeland hydrology and erosion model. *Transactions of the American Society of Agricultural and Biological Engineers* 54:901-908.
- Nicks, A., L. Lane, and G. Gander. 1995. Weather generator. Chapter 2. In *USDA—Water Erosion Prediction Project: Hillslope profile and watershed model documentation*, ed. D.C. Flanagan and M.A. Nearing. NSERL Report. West Lafayette, IN: USDA Agricultural Research Service National Soil Erosion Research Laboratory.
- Nouwakpo, S.K., and C.H. Huang. 2012. The role of subsurface hydrology in soil erosion and channel network development on a laboratory hillslope. *Soil Science Society of America Journal* 76:1197-1211.
- Okin, G.S., A.J. Parsons, J. Wainwright, J.E. Herrick, B.T. Bestelmeyer, D.C. Peters, and E.L. Fredrickson. 2009. Do Changes in Connectivity Explain Desertification? *Bioscience* 59:237-244.
- Osterkamp, W., P. Heilman, and L. Lane. 1998. Economic considerations of a continental sediment-monitoring program. *International Journal of Sediment Research* 13:12-24.
- Paige, G.B., J.J. Stone, J.R. Smith, and J.R. Kennedy. 2004. The walnut gulch rainfall simulator: A computer-controlled variable intensity rainfall simulator. *Applied Engineering in Agriculture* 20:25-31.
- Pierson, F.B., W.H. Blackburn, S.S. Van Vactor, and J.C. Wood. 1994. Partitioning small scale spatial variability of runoff and erosion on sagebrush rangeland. *Water Resources Bulletin* 30:1081-1089.
- Pierson, F.B., C.A. Moffet, C.J. Williams, S.P. Hardegre, and P.E. Clark. 2009. Prescribed-fire effects on rill and interrill runoff and erosion in a mountainous sagebrush landscape. *Earth Surface Processes and Landforms* 34:193-203.
- Pierson, F.B., P.R. Robichaud, C.A. Moffet, K.E. Spaeth, S.P. Hardegre, P.E. Clark, and C.J. Williams. 2008. Fire effects on rangeland hydrology and erosion in a steep sagebrush-dominated landscape. *Hydrological Processes* 22:2916-2929.
- Pierson, F.B., K.E. Spaeth, M.A. Weltz, and D.H. Carlson. 2002. Hydrologic response of diverse western rangelands. *Journal of Range Management* 55:558-570.
- Pierson, F.B., C.J. Williams, S.P. Hardegre, M.A. Weltz, J.J. Stone, and P.E. Clark. 2011. Fire, plant invasions, and erosion events on western rangelands. *Rangeland Ecology and Management* 64:439-449.
- Pierson, F.B., C.J. Williams, P.R. Kormos, S.P. Hardegre, P.E. Clark, and B.M. Rau. 2010. Hydrologic Vulnerability of Sagebrush Steppe Following Pinyon and Juniper Encroachment. *Rangeland Ecology and Management* 63:614-629.
- Puigdefabregas, J. 2005. The role of vegetation patterns in structuring runoff and sediment fluxes in drylands. *Earth Surface Processes and Landforms* 30:133-147.
- R Development Core Team. 2015. R: A Language and Environment for Statistical Computing, R Foundation for Statistical Computing, Vienna, Austria. <http://www.r-project.org/>.
- Ravi, S., P. D'Odorico, T.E. Huxman, and S.L. Collins. 2010. Interactions between soil erosion processes and fires: Implications for the dynamics of fertility islands. *Rangeland Ecology and Management* 63:267-274.
- Reaney, S.M., L.J. Bracken, and M.J. Kirkby. 2007. Use of the Connectivity of Runoff Model (CRUM) to investigate the influence of storm characteristics on runoff generation and connectivity in semiarid areas. *Hydrological Processes* 21:894-906.
- Reid, K.D., B.P. Wilcox, D.D. Breshears, and L. MacDonald. 1999. Runoff and erosion in a piñon-juniper woodland influence of vegetation patches. *Soil Science Society of America Journal* 63:1869-1879.
- Renard, K.G. 1970. The hydrology of semiarid rangeland watersheds. USDA Publication 01/1970; 41.
- Renard, K.G., G.R. Foster, G.A. Weesies, D. McCool, and D. Yoder. 1997. Predicting soil erosion by water: A guide to conservation planning with the revised universal soil loss equation (RUSLE). Agriculture Handbook. Washington, DC: US Government Printing Office.
- Renard, K.G., G.R. Foster, G.A. Weesies, and J.P. Porter. 1991. RUSLE: Revised Universal Soil Loss Equation. *Journal of Soil and Water Conservation* 46(1):30-33.
- Ridolfi, L., F. Laio, and P. D'Odorico. 2008. Fertility island formation and evolution in dryland ecosystems. *Ecology and Society* 13:13.
- Rieke-Zapp, D.H., and M.A. Nearing. 2005. Digital close range photogrammetry for measurement of soil erosion. *The Photogrammetric Record* 20:69-87.

- Ross, M. 2013. Using the rangeland hydrology and erosion model to assess rangeland management practices on the kaler ranch. Master's thesis, The University of Arizona.
- Saco, P.M., G.R. Willgoose, and G.R. Hancock. 2007. Eco-geomorphology of banded vegetation patterns in arid and semiarid regions. *Hydrology and Earth System Sciences* 11:1717-1730.
- Schlesinger, W.H., and A.M. Pilmanis. 1998. Plant-soil interactions in deserts. *Biogeochemistry* 42:169-187.
- Schlesinger, W.H., J.A. Raikes, A.E. Hartley, and A.E. Cross. 1996. On the spatial pattern of soil nutrients in desert ecosystems. *Ecology* 77:364-374.
- Shainberg, I., A.I. Mamedov, and G.J. Levy. 2003. Role of wetting rate and rain energy in seal formation and erosion 1. *Soil Science* 168:54-62.
- Spaeth, K.E., M.A. Wetz, H.D. Fox, and E.B. Pierson. 1994. Spatial Pattern Analysis of Sagebrush Vegetation and Potential Influences on Hydrology and Erosion. *In* Variability in Rangeland Water Erosion Processes, ed. W.H. Blackburn, E.B. Pierson, G.E. Schuman, and R. Zartman, p. 35-50. Madison, WI: Soil Science Society of America.
- Tongway, D.J., and B. Ludwig. 1997. The nature of landscape dysfunction in rangelands. *In* Landscape Ecology, Function and Management: Principles from Australia's Rangelands, ed. B. Ludwig, D. J. Tongway, D. Freudenberger, J. Noble, and K. C. Hodgkinson, p. 49-61. Melbourne, Australia: The Commonwealth Scientific and Industrial Research Organisation.
- Toy, T.J., and G.R. Foster. 1998. Guidelines for the use of the Revised Universal Soil Loss Equation (RUSLE) Version 1.06 on mined lands. Denver, CO: Construction Sites, and Reclaimed Lands, Western Regional Coordinating Center, Office of Surface Mining.
- Toy, T.J., G.R. Foster, and K.G. Renard. 1999. RUSLE for mining, construction and reclamation lands. *Journal of Soil and Water Conservation* 54(2):462-467.
- Trieste, D.J., and G.F. Gifford. 1980. Application of the Universal Soil Loss Equation to rangelands on a per-storm basis. *Journal of Range Management* 33:66-70.
- Truman, C.C., J.M. Bradford, and J.E. Ferris. 1990. Antecedent water content and rainfall energy influence on soil aggregates breakdown. *Soil Science Society of America Journal* 54:1385-1392.
- USDA ARS (Agricultural Research Service). 2014. Rangeland Hydrology and Erosion Model version 2.2 Equation summary. Tucson, AZ. <http://apps.tucson.ars.ag.gov/rhem/docs>.
- Valentin, C., J.M. d'Herbes, and J. Poesen. 1999. Soil and water components of banded vegetation patterns. *Catena* 37:1-24.
- VanAmburg, L., D. Booth, M. Wetz, and M. Trlica. 2005. A laser point frame to measure cover. *Rangeland Ecology & Management* 58:557-560.
- Wells, S.G., L.D. McFadden, and J.C. Dohrenwend. 1987. Influence of late quaternary climatic changes on geomorphic and pedogenic processes on a desert piedmont, Eastern Mojave Desert, California. *Quaternary Research* 27:130-146.
- Wetz, M.A., L. Jolley, M. Hernandez, K.E. Spaeth, C. Rossi, C. Talbot, M. Nearing, J. Stone, D. Goodrich, E. Pierson, H. Wei, and C. Morris. 2014a. Estimating conservation needs for rangelands using National Resources Inventory assessments. *Transactions of the American Society of Agricultural and Biological Engineers* 57:1559-1570.
- Wetz, M., and K. Spaeth. 2012. Estimating effects of targeted conservation on nonfederal rangelands. *Rangelands* 34:35-40.
- Wetz, M.A., K. Spaeth, M.H. Taylor, K. Rollins, E. Pierson, L. Jolley, M. Nearing, D. Goodrich, M. Hernandez, S.K. Nouwakpo, and C. Rossi. 2014b. Cheatgrass invasion and woody species encroachment in the Great Basin: Benefits of conservation. *Journal of Soil and Water Conservation* 69(2):39A-44A, doi:10.2489/jswc.69.2.39A.
- Wilcox, B.P., D.D. Breshears, and C.D. Allen. 2003. Ecohydrology of a resource-conserving semiarid woodland: Effects of scale and disturbance. *Ecological Monographs* 73:223-239.
- Williams, C.J., E.B. Pierson, O.Z. Al-Hamdan, P.R. Kormos, S.P. Hardegree, and P.E. Clark. 2014. Can wildfire serve as an ecohydrologic threshold-reversal mechanism on juniper-encroached shrublands. *Ecohydrology* 7:453-477.
- Zhang, Y., M. Hernandez, E. Anson, M.A. Nearing, H. Wei, J.J. Stone, and P. Heilman. 2012. Modeling climate change effects on runoff and soil erosion in southeastern Arizona rangelands and implications for mitigation with conservation practices. *Journal of Soil and Water Conservation* 67(5):390-405, doi:10.2489/jswc.67.5.390.